Desalination and Water Treatment
www.deswater.com

doi:10.5004/dwt.2016.0298

59 (2017) 82–88
January

Influence of seawater temperature on thermal efficiency of an integrated electric power generation and water desalination plant

Murat Tunc[a], Sedat Sisbot[b,*]

[a]*Istanbul Bilgi University, Engineering Faculty, Department of Energy Systems Engineering, 34060 Eyup, Istanbul, Turkey, email: murat.tunc@bilgi.edu.tr*
[b]*Izmir University, Faculty of Engineering, Department of Electronics and Communication, 35350, Uckuyular, Izmir, Turkey, Tel. +90 232 446 4949; email: sedat.sisbot@izmir.edu.tr*

Received 17 March 2016; Accepted 19 June 2016

ABSTRACT

This paper is an attempt to demonstrate the effect of sea water temperature on the overall efficiency of electric power generation combined with a water desalination plant. The plant under consideration is composed of two thermally and mechanically coupled loops: a steam power plant loop to produce electricity and a reverse osmosis loop including pressure exchange system to provide drinkable water from seawater. The reverse osmosis loop including pressure exchange system is known to be the state of the art desalination technology for obtaining fresh water. The waste pressure from reverse osmosis is transferred to the low pressure concentrate in a pressure exchange system to save a considerable amount of energy. It is shown in the body of paper that the sea water inlet temperature has a direct impact on the overall efficiency of the system. This is fundamentally accomplished by the rejected heat of Rankine cycle in a condenser. As a result, this paper shows that the overall efficiency of the combined plant is found to be highest when sea water temperature at the condenser exit is elevated to around 30°C.

Keywords: Combined electric power generation and desalination; Pressure exchange system; Seawater thermal efficiency; Water desalination; Reverse osmosis

1. Introduction

The demand for fresh water is dramatically increasing as a consequence of many contributing factors such as rapid growth in population, accelerated urbanization, global warming, improvement in living standards, increasing development of industrial and agricultural activities [1–3]. Fresh water represents only 3% (about 36 million km^3) of the earth's total water supply while another 97% is seawater of the oceans. 77% of the fresh water is locked in icecaps and glaciers, 22% of the fresh water underlies the earth's surface but much of it is too deep to access in an economically efficient manner. Then, readily available fresh-water resources from rivers, lakes and groundwater accounts for less than 1% [4–6]. Therefore, the shortage of fresh water resources and great demand for fresh water has become a serious issue for many countries [4]. The limited fresh water resources are being increasingly depleted at an alarming rate in many countries especially in the Middle East and North Africa [1–4,6]. It is therefore evident that removing salt from the virtually unlimited supply of seawater should play an important role in increasing the fresh water supply. Desalination has emerged as an important and dependable technology for obtaining fresh water from seawater in coastal regions [2,6–8].

Today, some countries greatly depend on desalination technologies for their fresh water requirements [3,7]. For example, in the Middle East countries like Saudi Arabia, United Arab Emirates and Kuwait, desalination plants are the primary source of fresh water. The top five countries sharing 60% of the desalinated fresh water are given in Table 1. [7–9].

There are several desalination technologies, such as multi- effect distillation (MED), reverse osmosis (RO), mul-

---

*Corresponding author.

1944-3994 / 1944-3986

Table 1
The top five countries where maximum desalination plant is located [9].

Saudi Arabia	17.4%
United States of America	16.2%
United Arab Emirates	14.7%
Spain	6.4%
Kuwait	5.8%

tiple stage flash (MSF), nanofiltration (NF), electrodialysis (EDR), vapor compression (VC) and low temperature multiple effect evaporation (LT-MEE) [1,4,10–13]. Among these, reverse osmosis (RO) is one of the most energy efficient and widely used technique [14,15]. This technology represents 42% of total installed desalination capacity throughout the world [7,16,17]. By means of this technique, salt concentrations below 3% (30,000 ppm) with a high water recovery rates can be achieved [7,18].

Most of the desalination processes consume high amounts of energy and the increase of desalinated water supply will cause serious problems such as high energy consumption and environmental pollution caused by the use of fossil fuels. The required energy for these systems can be reduced by combining the desalination plants with power plants. The dual purpose power desalination plants make use of the thermal energy extracted or exhausted from power plants as a alternative source of energy in thermal desalination processes. Therefore, many researchers have focused on the integration of desalination plants with power generation in the same site since these cogenerated plants deliver substantial cost savings in both the production of electricity and fresh water [8,10,11,15,19–22]. Several studies have been proposed in literature about dual-purpose configurations like; organic rankine cycle (ORC) for RO desalination [8,10,23–25], multiple effect distillation (MED) integrated with thermal vapour compression (TVC) [4,26], combined gas turbine and multi stage flash (MSF) desalination plant [11,21], the exhaust gas of IC engine for desalination [27], solar field driven organic rankine cycle (SORC) coupled with a desalination unit [28], triple hybrid power–MSF–RO system [4,22], etc.

Nearly all energy recovery systems incorporated in reverse osmosis plants are based on hydraulic turbines [29]. By application of a pressure exchange system (PES) which has already been in use in some other areas, a considerably energy efficiency might be achieved in reverse osmosis (RO) systems [7,30]. Technical details of the PES were presented in where the authors compared different energy recovery methods and concluded that PES was more efficient than that of alternating technologies using reverse running pumps or turbines [7,13,29,31–33]. The PES is well suited for large plants and it enables a simple variable adaption of discharge volume. Due to its design and direct pressure transmission of high pressure brine to the feed, the efficiency of this system can reach up to 98% and hence the incorporation of this technique in an RO plant can reduce its energy consumption by as much as 75% [31–34]. Agashichev and Lootah [13] proposed a model that permits analysis of the influence of temperature on osmotic pressure recovery and net energy consumption.

Generation of electricity and water using thermal desalination technologies integrated into the power plant process and the combination of such systems with more flexible sea water reverse osmosis membrane technology shows a great promise for advancing seawater desalination [35,36]. Despite that many contributions dealing with the development of dual purpose desalination configurations have been proposed in recent years, only few of them focus on the optimization of the configuration and operating conditions of these coupled systems. The temperature rise of seawater in the condenser is one of the non-negligible process parameter and it is essential to consider the effects of the seawater temperature increase on the thermal efficiency of the dual purpose desalination plants [10,22].

In this study, an integrated system using reverse osmosis to produce drinkable water and a Rankine cycle to generate electricity as well as to produce mechanical power to the pumps of the RO subsystem is examined. The effect of a pressure exchange system on RO efficiency via overall efficiency is also discussed. Heat rejected by the condenser of the Rankine cycle is used to heat up the seawater in a heat exchanger. A significant amount of energy economy has been obtained both by using the rejected heat from the condenser, which is used to heat up the seawater in a heat exchanger, and by using PES such that the expensive pressure energy from a high pressure fluid stream is transferred to a low pressure fluid stream in the pressure exchanger.

2. Model description

A functional block diagram of power and water cogeneration is given in Fig. 1. The power plant and reverse osmosis subsystems are coupled both mechanically and thermally. Heat produced in the Rankine cycle is used for seawater heating. The heat to be rejected is used to warm up the seawater.

The pressure exchange system transfers pressure energy from a high pressure fluid stream to low pressure fluid stream. As shown in Fig. 2, the way of providing a high pressure fluid in the PES is to transfer the waste pressure to a low pressure stream using a pressure exchanger. The working cycle of the PES chamber is activated and controlled by the valves. First, the chamber is filled with seawater at low pressure and then the seawater in the chamber is pressurized by applying the operating pressure of the concentrate. Then the seawater is moved from the chamber into the desalination modules by the concentrate entering the chamber at high pressure. This step is halted when all the feed has left the chamber or the chamber is filled completely with concentrate. Next the chamber is depressurized and seawater is pumped into the chamber that displaces the concentrate flowing to the discharge [37].

When the chamber is completely filled with seawater, a new cycle is initiated with the pressurization by the concentrate and the displacement of the content. When a single chamber is used, the system renders discontinuous operation. In order to avoid discontinuity three chambers are employed such that the content of one of the chambers is always available at the output. Therefore, a continuous

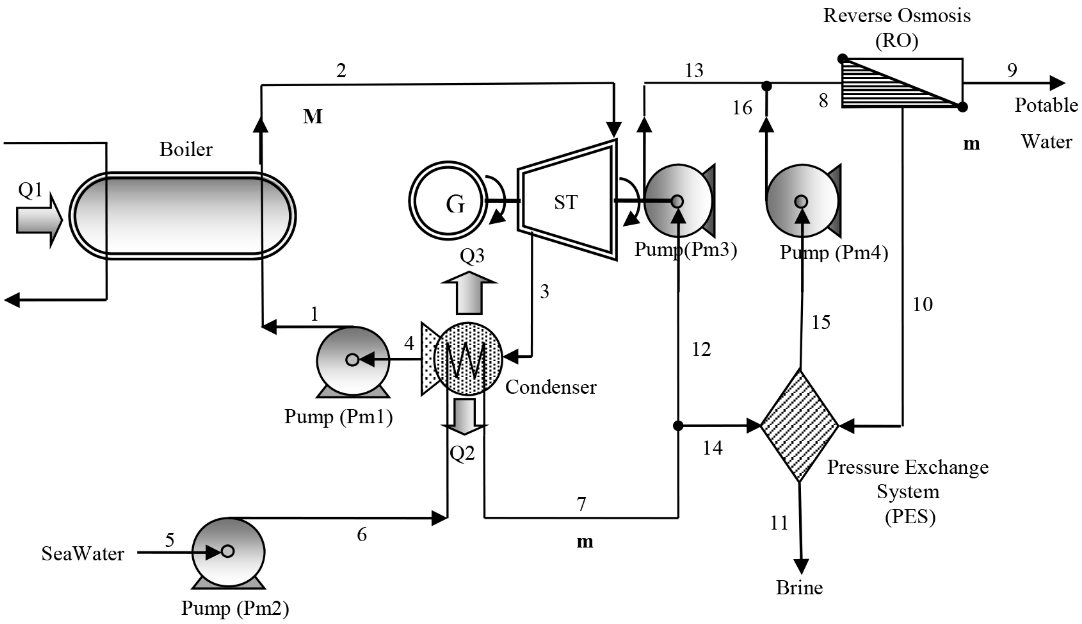

Fig. 1. Schematic diagram of power and water cogeneration by RO with PES and thermal coupling.

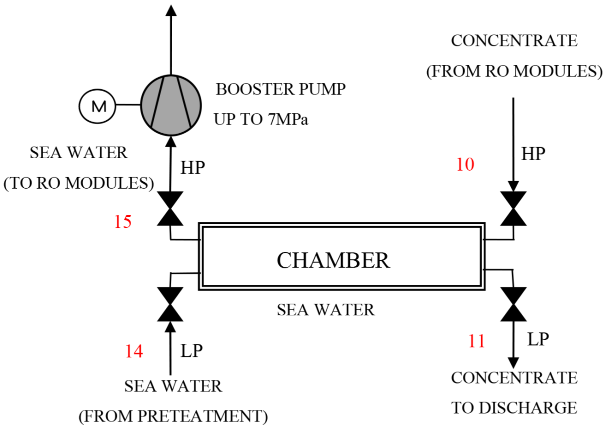

Fig. 2. Scheme of PES.

input and output operation can be achieved. Besides the high efficiency reaching up to 98% for the power conversion, PES has a flexible structure, the chamber's volume and pressure can be adapted to RO plants with two and more desalination trains. This adaption is accomplished by the automatic controlling of the system parameters [37–39].

The following assumptions have been made for our model considering process diagram in Fig.1 [7,24].

- Water, salt and saline solutions are incompressible substances.
- Kinetic and potential energies are negligible at all stages.
- The conditions of the saltwater at the inlet (point 5) represent the reference state used to evaluate the exergy.
- Frictional pressure losses are neglected except in the pressure vessel of the RO subsystem.
- The flow is steady.
- Salinity at the entry (at point 5) is constant.
- The efficiencies of all pumps and turbines are fixed at the same value of 90%.
- The PES efficiency is fixed at a constant 90%.
- Pressure losses due to filters have been neglected.

The plant operating parameters taken into consideration for furthering part of the calculations are presented in Table 2.

The properties of the saltwater depend on its pressure, temperature and salinity. The salinity can be expressed in various forms as in parts per million (ppm) on a mass basis as a percentage (*salt*), a salt mass fraction (mf_s) or a salt mole fraction (x_s). Saltwater having less than 5% salinity is considered to be a dilute solution and can be treated as an ideal solution. Therefore its extensive properties are evaluated as a weighted average of the corresponding properties of its components [40–42].

Table 2
Operating parameters in Fig. 1 (*)

Environment	Rankine cycle	Reverse osmosis
	$q_1 = 3100$ kJ kg^{-1}	$P_8 = 6$ MPa
	$P_1 = P_2 = 4$ MPa	$\mu_{Pm1} = \mu_{Pm3} = \mu_{Pm4} = 90\%$
$P_9 = 101.13$ kPa	$P_6 = P_7 = 0.2$ MPa	$\mu_{PES} = 90\%$
$P_5 = P_9 = P_{11}$	$P_3 = P_4 = 15$ MPa	$\pi = 80\%$
$S_5 = 34000$ ppm $= 3.4\%$	$T_2 = 450°C$	

(*) Subscripts are the points shown in Fig.1

The specific heat and enthalpy of salt water can be given by,

$$C_{p,Sw} = (1 - mf_S)C_{p,W} + mf_S C_{p,S} \tag{1}$$

$$h_{Sw} = (1 - mf_S)h_W + mf_S h_S \tag{2}$$

Since mixing is an irreversible process, the entropy of a mixture is greater than the weighted sum of the entropies of its components. Hence the entropy of salt water is given by,

$$s_{sw} = (1 - mf_S)s_w + mf_S s_S \tag{3}$$

Thermodynamic properties of salt, NaCl, at T = 15°C are given as follows,

$C_{p,s} = 0.8368$ kJ/kgK

$h_{S0} = 12.552$ kJ/kg

$s_{S0} = 0.04473$ kJ/kgK

$V_{NaCl} = 1/\rho = 1/2165 = 0.0004618\ \text{m}^3\ \text{kg}^{-1}$

$C_{pwater} = 1.8368$ kJ/kgK

By substituting into the above equations, the following set of results was obtained:

$h_S = h_{S0} + C_{p,S}\,(T - T_0) = 12.552 + 0.8368(T - 288)$

$s_S = s_{S0} + C_{p,S}\,ln(T/T_0) = 0.04473 + 0.83686\ ln(T/288)$

$C_{p,sw5} = 0.95 \times 4.23 + 0.05 \times 0.8368 = 4.06$ kJ/kgK

$C_{sw5} = 0.95 \times 62.99 + 0.05 \times 12.552 = 60.46$ kJ/kgK

$S_{sw5} = 0.95 \times 0.2245 + 0.05 \times 0.04473 = 0.2155$ kJ/kgK

$v_{sw5} = 0.95 \times 0.001001 + 0.05 \times 0.0004618 = 0.000974\ m^3/kg$

3. Thermal analysis and evaluation

Thermodynamic equations for a given system in steady flow are expressed as follows:

Mass balance equation:

$$\sum_{in} m = \sum_{out} m \tag{4}$$

The overall energy balance is:

$$Q + \sum_{in} mh = W + \sum_{out} mh \tag{5}$$

$$Q_1 + m_5 h_5 = Q_3 + m_9 h_9 + m_{11} h_{11} + W_G \tag{6}$$

Similarly, the energy balance equation for power plant is:

$$Q_1 = Q_2 + Q_3 + W_{ST} - W_{Pm1} \tag{7}$$

By combining these two relations given in Eqn. (6) and (7) and using the expressions for mass and energy conservation for the individual components, which make up the system and dividing by power plant mass flow rate M, the following expression for the system was obtained.

$$\frac{W_G}{M} = W_{ST} - W_{P1} - \left(\frac{W_{P2}}{r_3}\right) - \left(\frac{W_{P3}}{r_3}\right) - \left(\frac{r_2}{r_3}\right) W_{P4} \tag{8}$$

where

$r_1 = m_9/m_5$: Permeate recovery ratio

$r_2 = m_{11}/m_5$: Brine rejection ratio

$r_3 = M/m_5$: Power plant mass ratio

The difference between B_{in} and B_{out} is the rate of exergy destruction, $B_{det.t,}$ as,

$$B_{in,t} - B_{out.t} = B_{det.t} \tag{9}$$

The exergy or the second law efficiency of the systems is,

$$\mu_{ex} = \frac{B_{out.t}}{B_{in.t}} = 1 - \frac{B_{det.t}}{B_{in.t}} \tag{10}$$

The total exergy input per unit mass of feed water is defined as,

$$B_{in.t} = r_3\left(1 - \frac{T_0}{T_s}\right) q_1 \tag{11}$$

The corresponding total destroyed exergy can then be expressed as,

$$\begin{aligned} B_{det.t} = {} & r_3\left(\underset{boil}{B_{det}} + \underset{vt}{B_{det}} + \underset{P1}{B_{det}} + \underset{cond}{B_{det}}\right) + r_2\left(\underset{PES}{B_{det}} + \underset{P4}{B_{det}}\right) \\ & + r_1\left(\underset{P3}{B_{det}} + \underset{P2}{B_{det}} + \underset{RO}{B_{det}}\right) \end{aligned} \tag{12}$$

The attainable upper value of recovery is restricted by physical limits, namely, resistance due to the osmotic pressure. The maximum value of osmotic pressure, π_{max}, is assumed to be at outlet concentration, $C_{CONCENTRATE}$, of a high pressure channel [13].

$$\pi < \pi_{MAX}\left(\pi_{MAX} = C_{CONCENTRATE}\right) \tag{13}$$

$$\begin{aligned} Q_{FEED}\ C_{FEED} = {} & Q_{PERMEATE}\ C_{PERMEATE} \\ & + Q_{CONCENTRATE}\ C_{CONCENTRATE} \end{aligned} \tag{14}$$

For the outlet concentration $C_{CONCENTRATE}$ to be estimated, a mass balance equation for a semi-permeable channel (Eq. (15)) can be used. Assuming that trans-membrane flux rejection, R_M, and transport characteristic are position-independent and constant along the membrane surface, Eq. (15) can be rewritten in terms of recovery and membrane rejection as follows,

Table 3
The changes of temperature and salinity of potable water depends on r_3

r_3	T_8	r_1	μ_{ex}	S_9 (%)	W_G
0.30	17.67	30.87	1.13	0.07496	0.00
0.40	18.17	31.15	9.73	0.07592	9.56
0.50	18.67	31.43	16.24	0.07689	32.73
0.60	19.17	31.71	20.58	0.07786	239.01
0.70	19.67	31.99	23.69	0.07885	386.36
0.80	20.17	32.27	26.01	0.07984	496.87
0.90	20.67	32.55	27.82	0.08083	582.82
1.00	21.17	32.83	29.27	0.08184	651.58
1.10	21.67	33.11	30.45	0.08285	707.84
1.20	22.17	33.39	31.44	0.08387	754.72
1.30	22.67	33.67	32.28	0.08490	794.39
1.40	23.17	33.95	32.99	0.08594	828.39
1.50	23.67	34.23	33.61	0.08698	857.86
1.60	24.17	34.51	34.16	0.08804	883.64
1.70	24.67	34.79	34.64	0.08910	906.40
1.80	25.17	35.07	35.06	0.09017	926.62
1.90	25.67	35.35	35.44	0.09125	944.71
2.00	26.17	35.63	35.79	0.09234	961.00
2.10	26.67	35.91	36.10	0.09344	975.73
2.20	27.17	36.19	36.38	0.09455	989.13
2.30	27.67	36.47	36.63	0.09566	1001.36
2.40	28.17	36.75	36.87	0.09679	1012.57
2.50	28.67	37.03	37.09	0.09792	1022.88
2.60	29.17	37.31	37.29	0.09907	1032.40
2.70	29.67	37.59	37.47	0.10022	1041.22
2.80	30.17	37.87	37.65	0.10139	1049.41
2.90	30.67	38.15	37.81	0.10256	1057.03
3.00	31.17	38.43	37.96	0.10375	1064.14
3.10	31.17	37.95	38.10	0.10375	1070.80
3.20	31.17	37.95	38.23	0.10375	1076.98

$$Q_{FEED}\,C_{FEED} = Q_{FEED}\,C_{FEED}\left(1-R_M\right) + Q_{FEED}\left(1-r_1\right)C_{CONCENTRATE} \tag{15}$$

By solving Eq. (16) for $C_{CONCENTRATE}$ the outlet concentration as a function of permeate recovery r_1 and rejection R_M was obtained. The concentration is assumed to be constant throughout the cross section.

$$C_{CONCENTRATE} = C_{FEED}\left\{1-\frac{\left[1-r_1\left(1-R_M\right)\right]}{\left[1-r_1\right]}\right\} \tag{16}$$

4. Results and Discussion

Mechanically and thermally coupled power plants combined with reverse osmosis systems was examined. The rejected heat of the cycle is used to warm up the sea water in the condenser. In Table 3, various values of elevated sea water temperature after condenser with respect to r_1, r_2, S_9 (salt), μ_{ex} (exergy efficiency) and W_G (obtained work from generator) have been presented. In this respect r_1 represents the ratio of permeate to sea water mass flow rates, r_3 is the ratio of power plant mass flow rate over sea water mass flow rate. T_8 and r_1 both increase simultaneously. It can be seen from Table 3 that r_1 declines when sea water temperature is around 30°C.

It can be seen from Table 3 that the increase of salinity of potable water with the increase of temperature. However, the salinity of water should approximately be 0.1% or 1000 ppm for it to be drinkable. So, heat transfer in the condenser should permit the increase of the operating temperature of the reverse osmosis (RO) unit, which in turn increases the quantity of potable water produced to an optimum temperature. The variation of versus elevated sea water temperature is given in Fig. 3. Salinity of potable water versus sea water temperature is depicted in the Fig. 4. It can also be seen from Fig. 4 that the salinity of potable water is directly proportional with sea water temperature. The viscosity of the feed water is strongly depends on its temperature. As the temperature increases, water viscosity decreases and the RO membrane becomes more permeable, with a consequent increase in production. However, there is also a simultaneous enhancement in the rate of salt diffusion with the rising temperature, leading to a slight increase in product water salinity. When selecting the optimum temperature of the RO these aspects should be taken into account. Sea water temperature versus exergy efficiency is given in the Fig. 5. The second law efficiency reaches its maximum value at sea water temperature of 30°C, at which the permeate recovery ratio reaches to its maximum value as shown in the Fig. 3.

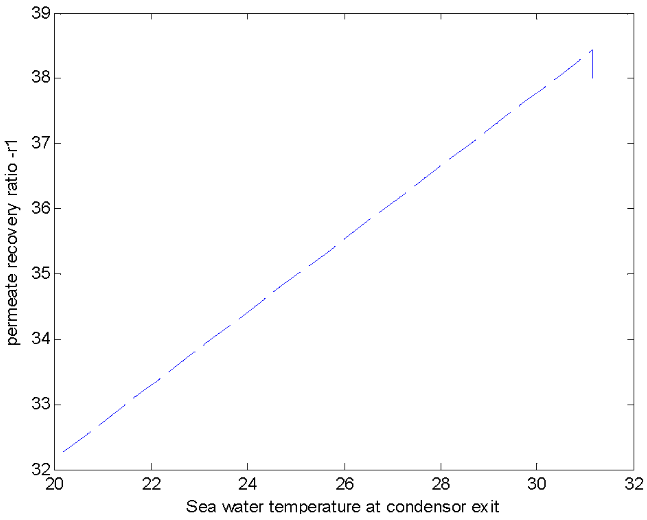

Fig. 3. Sea water temperature changes versus permeate recovery ratio r_1.

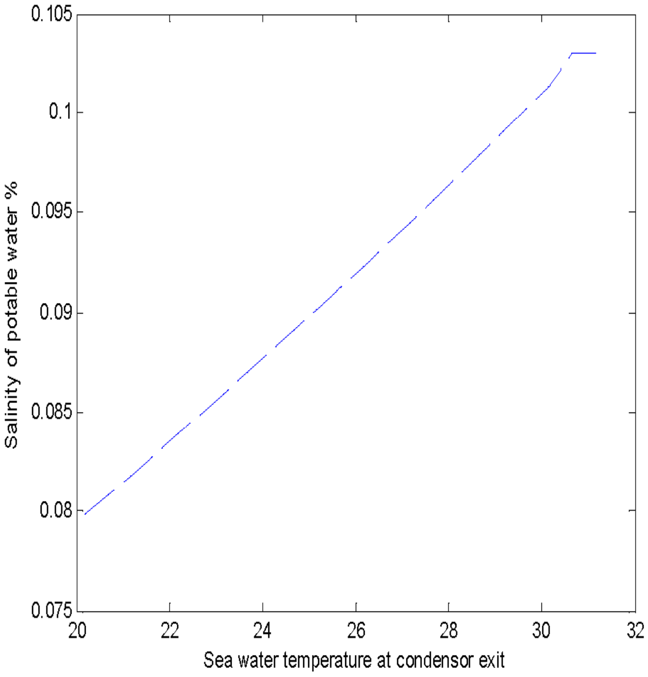

Fig. 4. Temperature versus permeate salinity.

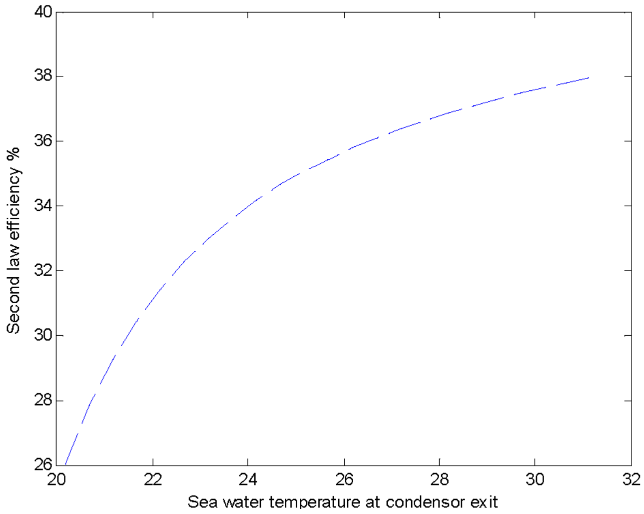

Fig. 5. Second law efficiency versus temperature.

Another topic of concern is the cost of such process. The cogeneration plants for simultaneous production of water and electricity have proven to be more thermodynamically efficient and economically lucrative than single purpose power generation and water production plants. The unit production costs of water and electricity of the cogeneration cycle for an integrated water/power plant are given as \$0.433/m^3 and \$0.00844/kWh, respectively by Hamed O.A et al. [43]. Increasing sea water temperature to 30°C at the condenser exit, it is predicted a 3% drop in the amortized capital cost for water production and power generation values which are obtained as \$0.420/m^3 and \$0.00819/kWh, respectively.

Nomenclature

C_p — Specific heat (J kg^{-1} K^{-1})
B — Exergy (J)
P — Pressure (Pa)
h — Enthalpy (J kg^{-1})
M — Mass flow rate in power plant (kg s^{-1})
m — Saltwater mass flow rate (kg s^{-1})
mf — Mass fraction (kg kg^{-1})
q — Heat transfer per unit mass (W kg^{-1})
r_1 — Permeate recovery ratio (m_9/m_5)
r_2 — Brine rejection ratio (m_{11}/m_5)
r_3 — Power plant mass ratio (M/m_5)
s — Entropy (J kg^{-1} K^{-1})
Q — Rate of heat transfer (W)
T — Temperature (°C)
v — Specific volume (m^3 kg^{-1})
w — Work per unit mass (J kg^{-1})
x — Molar fraction (mol mol^{-1})
η — Efficiency (%)
W — Power (W)
π — Osmotic pressure (bar)
ρ — Density (kg m^{-3})
S — Salt (ppm)
sw — Salt water
R_M — Trans-membrane flux rejection
PES — Pressure exchange system
RO — Reverse osmosis
ST — Steam turbine
G — Electric generator

5. Conclusion

The overall steady state performance of an electric power generation integrated with water desalination plant has been investigated. Emphasis is given to the significance of the thermal efficiency of sea water temperature. From the desalination point of view, maximizing , permeate recovery ratio, and minimizing salt percentage is an optimum operating condition. It is considered that the sea water is being heated in the condenser by the rejected heat of the Rankine cycle. The optimum value is reached when sea water temperature is 31.17°C at which the overall system has reached the maximum exergy efficiency under the assumed conditions. The combined system also renders a 3% amortized capital cost reduction.

References

[1] S. Zhou, Y. Guo, X. Mu, S. Shen, Effect of design parameters on thermodynamic losses of the heat transfer process in LT-MEE desalination plant, Desalination, 375 (2015) 40–47.
[2] K.M. Bataineh, Multi-effect desalination plant combined with thermal compressor driven by steam generated by solar energy, Desalination, 385 (2016) 39–52.
[3] Q. Chun-hua, F. Hou-jun, L. Qing-chun, X. Yu-lei, L. Nan, Performance study of a pilot-scale low-temperature multi-effect desalination plant, Appl. Energy, 135 (2014) 415–422.
[4] M.T. Mazini, A. Yazdizadeh, M.H. Ramezani, Dynamic modeling of multi-effect desalination with thermal vapor compressor plant, Desalination, 353 (2014) 98–108.
[5] A.D. Khawaji, I.K. Kutubkhanah, J.M. Wie, Advances in seawater desalination technologies, Desalination, 221 (2008) 48–52.

[6] I.C. Watson, and O.J. Morin, Desalination and Water Purification Research and Development Program. Desalting Handbook for Planners (2003) Report No. 72. Florida.

[7] N. Bouzayani, N. Galanis, J. Orfi, Thermodynamic analysis of combined electric power generation and water desalination plants, Appl. Thermal Eng., 29 (2009) 624–633.

[8] A.S. Nafey, and M.A. Sharaf, Combined solar organic Rankine cycle with reverse osmosis desalination process: Energy, exergy, and cost evaluations, Renew. Energy, 35 (2010) 2571–2580.

[9] A.A. Alawadhi, Regional Report on Desalination- GCC Countries in: Proceedings of the IDA World Congress on Desalination and Water Reuse (2002) Manama. Bahrain. 8–13.

[10] D. Geng, Y. Du, R. Yang, Performance analysis of an organic Rankine cycle for a reverse osmosis desalination system using zeotropic mixtures, Desalination, 381 (2016) 38–46.

[11] S.R. Hosseini, M. Amidpour, A. Behbahaninia, Thermoeconomic analysis with reliability consideration of a combined power and multi stage flash desalination plant, Desalination, 278 (2011) 424–433.

[12] R. Deng, L. Xie, H. Lin, J. Liu, W. Han, Integration of thermal energy and seawater desalination, Energy, 35 (2010) 4368–4374.

[13] S.P. Agashichev, and K.N. Lootah, Influence of temperature and permeate recovery on energy consumption of a reverse osmosis system, Desalination, 154 (2003) 253–266.

[14] B.A. Qureshi, and S.M. Zubair, Exergetic efficiency of NF, RO and EDR desalination plants, Desalination, 378 (2016) 92–99.

[15] C. Li, S. Besarati, Y. Goswami, E. Stefanakos, H. Chen, Reverse osmosis desalination driven by low temperature supercritical organic rankine cycle, Appl. Energy, 102 (2013) 1071–1080.

[16] A. Altaee, and A. Sharif, Pressure retarded osmosis: advancement in the process applications or power generation and desalination, Desalination, 356(15) (2015) 31–46.

[17] O.K. Buros, The ABCs of Desalting. Second Ed. International Desalination Association (2003) Topsfield. MA. USA.

[18] A. Altaee, G.J. Millar, G. Zaragoza, Integration and optimization of pressure retarded osmosis with reverse osmosis for power generation and high efficiency desalination, Energy, 103 (2016) 110–118.

[19] V. Gadhamshetty, V.G. Gude, N. Nirmalakhandan, Thermal energy storage system for energy conservation and water desalination in power plants, Energy, 66 (2014) 938–949.

[20] A.H. Araghi, M. Khiadani, K. Hooman, A novel vacuum discharge thermal energy combined desalination and power generation system utilizing R290/R600a, Energy, 98 (2016) 215–224.

[21] Seyed Reza Hosseini, Majid Amidpour, Seyed Ehsan Shakib, Cost optimization of a combined power and water desalination plant with exergetic, environment and reliability consideration, Desalination, 285 (2012) 123–130.

[22] W. Lianying, H. Yangdong, G. Congjie, Optimum design of cogeneration for power and desalination to satisfy the demand of water and power, Desalination, 324 (2013) 111–117.

[23] G. Kosmadakis, D. Manolakos, S. Kyritsis, G. Papadakis, Design of a two stage organic Rankine cycle system for reverse osmosis desalination supplied from a steady thermal source, Desalination, 250 (2010) 323–328.

[24] M. Ameri, and M. Jorjani, Performance assessment and multi-objective optimization of an integrated organic Rankine cycle and multi-effect desalination system, Desalination, 392 (2016) 34–45.

[25] B.F. Tchanche*, Gr. Lambrinos, A. Frangoudakis, G. Papadakis, Exergy analysis of micro-organic Rankine power cycles for a small scale solar driven reverse osmosis desalination system, Appl. Energy 87 (2010) 1295–1306.

[26] A. Tamburini, A. Cipollina, G. Micale, A. Piacentino, CHP (combined heat and power) retrofit for a large MED-TVC (multiple effect distillation along with thermal vapour compression) desalination plant: high efficiency assessment for different design options under the current legislative EU framework, Energy, (2016) 1–12.

[27] K.S. Maheswari, K.K Murugavel, G. Esakkimuthu, Thermal desalination using diesel engine exhaust waste heat — An experimental analysis, Desalination, 358 (2015) 94–100.

[28] C. Li, G. Kosmadakis, D. Manolakos, E. Stefanakos, G. Papadakis, D.Y. Goswami, Performance investigation of concentrating solar collectors coupled with a transcritical organic Rankine cycle for power and seawater desalination co-generation, Desalination, 318 (2013) 107–117.

[29] S. Bross, and W. Kochanowski, SWRO core hydraulic module — The right concept decides in terms of energy consumption and reliability. Part II. Advanced pressure exchanger design, Desalination, 165 (2004) 351–361.

[30] N. Bouzayani, N. Galanis, J. Orfi, Comparative study of power and water cogeneration systems, Desalination, 205 (2007) 243–253.

[31] P. Geisler, F.U. Hahnenstein, W. Krumm, T. Peters, Pressure exchange system for energy recovery in reverse osmosis plants, Desalination, 122 (1999) 151–156.

[32] W. Zhou, L. Song, T.K. Guan, A numerical study on concentration polarization and system performance of spiral wound RO membrane modules, J. Membr. Sci., 271 (2006) 38–46.

[33] A. Altaee, G. Zaragoza, S. Adel, Pressure retarded osmosis for power generation and seawater desalination: Performance analysis, Desalination, 344 (2014) 108–115.

[34] A. Date, M. Ahmadi, A. Akbarzadeh, S. Ganguly, M.S. Kumar, Experimental Performance Investigation and Case Study of Combined Desalination and Power Generation. Proceedings World Geothermal Congress. Melbourne. Australia (2015) 19–25.

[35] H. Ludwig, Hybrid systems in seawater desalination—practical design aspects, present status and development perspectives, Desalination, 164 (2004) 1–18.

[36] W. He, Y. Wang, A. Sharif, M.H. Shaheed, Thermodynamic analysis of a stand-alone reverse osmosis desalination system powered by pressure retarded osmosis, Desalination, 352 (2014) 27–37.

[37] P. Geisler, W. Krumm, T. Peters, Optimization of the energy demand of reverse osmosis with a pressure-exchange system, Desalination, 125 (1–3) (1999) 167–172.

[38] A.S. Nafey, M.A. Sharaf, L. García-Rodríguez, Thermo-economic analysis of a combined solar organic Rankine cycle-reverse osmosis desalination process with different energy recovery configurations, Desalination, 261(1–2) (2010) 138–147.

[39] B. Peñate, L. García-Rodríguez, Retrofitting assessment of the Lanzarote IV seawater reverse osmosis desalination plant, Desalination, 266 (1–3) (2011) 244–255.

[40] Y.C. Kim, and M. Elimelech, Potential of osmotic power generation by pressure retarded osmosis using seawater as feed solution: Analysis and experiments, J. Membr. Sci., 429 (2013) 330–337.

[41] Y. Cerci, Exergy analysis of a reverse osmosis desalination plant in California, Desalination, 142 (2002) 257–266.

[42] R. Deng, L. Xie, H. Lin, J. Liu, W. Han, Integration of thermal energy and seawater desalination, Energy, 35(11) (2010) 4368–4374.

[43] O.A. Hamed, H.A. Al-Washmi, H.A. Al-Otaibi, Thermoeconomic analysis of a power/water cogeneration plant, Energy, 31(14) (2006) 2699–2709.